Journal of Applied Mathematics and Mechanics 72 (2008) 226–232

Contents lists available at ScienceDirect

Journal of Applied Mathematics and Mechanics

journal homepage: www.elsevier.com/locate/jappmathmech

Modelling of the deformation processes and the localization of plastic deformations in the torsion–tension of solids of revolution☆

V.G. Bazhenov, S.V. Zefirov, L.N. Kramarev, Ye.V. Pavlenkova

Nizhnii Novgorod, Russia

ARTICLE INFO

Article history:
Received 7 December 2006

ABSTRACT

Generalized two-dimensional problems of the torsion of elastoplastic solids of revolution of arbitrary shape for large deformations under non-uniform stress-strain conditions are formulated and a method for their numerical solution is proposed. The use of this method to construct strain diagrams of materials based on experiments on the torsion of axisysmmetric samples of variable thickness until fracture occurs is described. Experimental and numerical investigations of processes of elastoplastic deformation, loss of stability and supercritical behaviour of solid cylindrical steel samples of variable thickness under conditions of monotonic kinematic loading with a torque, a tension and a combined load are presented. The mutual influence of torsion and tension on the deformation process and the limit states is estimated, and the universality (the independence of the form of the stress-strain state) of the "stress intensity – Odqvist parameter" diagram for steel for large deformations is proved.

Traditionally, the mechanical properties of materials is determined from experiments on the stretching of samples. However, when investigating the strength characteristics difficulties arise due to the occurrence of non-uniaxiality and non-uniformity of the stress-strain state in the samples, due to non-linear boundary effects and localization of the deformations. When carrying out experiments on the torsion–tension of thin-walled cylindrical samples, loss of stability of the envelope precedes fracture. It is well known that the greatest uniform deformations occur under torsion in the surface layer of solid cylindrical samples.[1] The non-uniformity of the stress-strain state over the thickness of thick-walled samples makes it difficult to process the experimental data when determining the stress-strain state. Existing approaches to solving this problem – Ludwik's method[2] and the "conditional thin-walled tube" method[3] – impose limitations on the shape of the samples and assume that the stress-strain state is uniform over their length, which does not enable the stress-strain state to be estimated at the instant when fracture occurs.

To identify the strain and strength characteristics of materials under large elastoplastic deformations when the stress state is complex (torsion–tension) it is better to use methods of mathematical modelling of the deformation of laboratory samples or structural components. A variational-difference method of solving generalized two-dimensional torsion problems has been developed for this purpose, which enable the deformation of elastoplastic solids of revolution to be modelled under the combined action of an axisymmetric load and torsion, taking large deformations into account.

1. Numerical solution

When solving generalized two-dimensional torsion problems, we will start from the Jourdain principle of minimum work, written in a cylindrical system of coordinates r, β, z (Oz is the axis of revolution):

☆ *Prikl. Mat. Mekh.* Vol. 72, No. 2, pp. 342–350, 2008.
E-mail address: bazhenov@dk.mech.unn.ru (V.G. Bazhenov).

0021-8928/$ – see front matter © 2008 Elsevier Ltd. All rights reserved.
doi:10.1016/j.jappmathmech.2008.04.001

$$\iint_\Omega (\sigma_{rr}\delta\dot{e}_{rr} + \sigma_{\beta\beta}\delta\dot{e}_{\beta\beta} + \sigma_{zz}\delta\dot{e}_{zz} + 2\sigma_{rz}\delta\dot{e}_{rz} + \quad 2\sigma_{r\beta}\delta\dot{e}_{r\beta} + 2\sigma_{\beta z}\delta\dot{e}_{\beta z})rd\Omega +$$

$$+ \iint_\Omega (\rho w_r\delta\dot{u}_r + \rho w_\beta\delta\dot{u}_\beta + \rho w_z\delta\dot{u}_z)rd\Omega -$$

$$- \int_{G_p} (p_r\delta\dot{u}_r + p_\beta\delta\dot{u}_\beta + p_z\delta\dot{u}_z)rdG - \int_{G_q} (q_r\delta\dot{u}_r + q_\beta\delta\dot{u}_\beta + q_z\delta\dot{u}_z)rdG = 0 \tag{1.1}$$

where σ_{ij} and $\dot{e}_{ij}$ are the components of the Cauchy stress tensor and the rates of strain tensor, $\dot{u}_\alpha$ and w_α are the components of the displacement velocity and displacement acceleration vectors, p_α and q_α are the components of the surface and contact loads ($i, j, \alpha = r, \beta, z$), ρ is the density, Ω is the area occupied by the meridional section of the solid medium, G_p is the part of the surface on which the known surface load is specified a priori, and G_q is the part of the surface on which the contact pressures are specified in the course of the solution. By virtue of the axial symmetry, all the required functions depend on the radial and axial coordinates and do not depend on the circumferential coordinate.

The kinematic relations are formulated in velocities and are constructed in an actual-state metric, which enables us to take large deformations into account. The components of the rate of strain and rates of rotation tensors, taking into account the equality $\dot{u}_\beta = r\dot{\theta}$ (θ is the angle of torsion with respect to the circumferential coordinate β), have the form

$$\dot{e}_{rr} = \dot{u}_{r,r},\ \dot{e}_{\beta\beta} = \dot{u}_r r^{-1},\ \dot{e}_{zz} = \dot{u}_{z,z},\ \dot{e}_{zr} = \frac{1}{2}(\dot{u}_{z,r} + \dot{u}_{r,z}),\ \dot{e}_{r\beta} = \frac{1}{2}r\dot{\theta}_{,r},\ \dot{e}_{\beta z} = \frac{1}{2}r\dot{\theta}_{,z}$$

$$\dot{\omega}_{zr} = \frac{1}{2}(\dot{u}_{z,r} - \dot{u}_{r,z}),\quad \dot{\omega}_{r\beta} = -\frac{1}{2}(r\dot{\theta}_{,r} + 2\dot{\theta}),\quad \dot{\omega}_{\beta z} = \frac{1}{2}r\dot{\theta}_{,z} \tag{1.2}$$

To eliminate the singularity on the axis of revolution and to increase the accuracy of the numerical solution of the equations of motion, we introduce the following new functions

$$\dot{v}_r = r\dot{u}_r,\quad \dot{v}_z = r\dot{u}_z,\quad \dot{\theta} = r^{-1}\dot{u}_\beta$$

Then, the general equation of dynamics (1.1), taking relations (1.2) into account, can be converted to the form

$$-\iint_\Omega \left(\sigma_{rr}\frac{\partial\delta\dot{v}_r}{\partial r} + \sigma_{rz}\frac{\partial\delta\dot{v}_r}{\partial z} - \frac{\sigma_{rr} - \sigma_{\beta\beta}}{r}\delta\dot{v}_r + \rho w_r\delta\dot{v}_r\right)d\Omega - \int_G (p_r + q_r)\delta\dot{v}_r dG = 0$$

$$\iint_\Omega \left(\sigma_{r\beta}\frac{\partial\delta\dot{\theta}}{\partial r} + \sigma_{\beta z}\frac{\partial\delta\dot{\theta}}{\partial z} + \rho w_\beta\delta\dot{\theta}\right)r^2 d\Omega - \int_G (p_\beta + q_\beta)r^2\delta\dot{\theta}dG = 0$$

$$\iint_\Omega \left(\sigma_{zz}\frac{\partial\delta\dot{v}_z}{\partial z} + \sigma_{rz}\frac{\partial\delta\dot{v}_z}{\partial r} - \frac{\sigma_{rz}}{r}\delta\dot{v}_z + \rho w_z\delta\dot{v}_z\right)d\Omega - \int_G (p_z + q_z)\delta\dot{v}_z dG = 0 \tag{1.3}$$

The theory of flow with non-linear isotropic strengthening is used to describe the elastoplastic properties of materials. The relation between the components of the stress-rate deviator $\dot{\sigma}'_{ij} = \dot{\sigma}_{ij} + \dot{P}\delta_{ij}$ and elastic parts of the components of the strain-rate deviator $(\dot{e}^e_{ij})' = \dot{e}_{ij} - \dot{e}\delta_{ij}/3 - \dot{e}^p_{ij}$ is obtained using the generalized Hooke's law in the actual-state metric

$$D_J\sigma'_{ij} = 2G(\dot{e}^e_{ij})',\quad D_J\sigma'_{ij} = \dot{\sigma}'_{ij} - \dot{\omega}_{ik}\sigma'_{kj} - \dot{\omega}_{jk}\sigma'_{ik}$$

$$\dot{P} = -K\dot{e}^e,\quad \dot{P} = -\dot{\sigma}_{ii}/3,\quad \dot{e} = \dot{e}^e_{ii},\quad \dot{e}^p_{ii} = 0 \tag{1.4}$$

Here K and G are the bulk compression and shear moduli, P is the pressure, D_J is the Jaumann derivative, which describes the rotation of a particle of the medium as a rigid whole, and δ_{ij} is the Kronecker delta. Because of the axial symmetry we can ignore the total angle of rotation about the Oz axis in the expressions for the components of the rotation rates tensor $\dot{\omega}_{ij}$ (the last three equations of (1.2)). The plastic-strain rates are defined by the associated flow law

$$\dot{e}^p_{ij} = \dot{\lambda}\sigma'_{ij},\quad \sigma'_{ij}\sigma'_{ij} = \frac{2}{3}\sigma_i^2(\kappa),\quad \kappa = \sqrt{\frac{2}{3}}\int_0^t \sqrt{\dot{e}^p_{ij}\dot{e}^p_{ij}}dt \tag{1.5}$$

The system of equations (1.2)–(1.5), supplemented by the kinematic boundary and initial conditions, represents the complete formulation of the initial-boundary-value problem. For numerical modelling, the calculation region is approximated by a Lagrange net of four-node elements. The components of the displacement, rate of displacement and acceleration vectors are determined at the grid nodes, while the components of the stress and strain tensors are determined at the centres of the elements.[4] Replacing the integration over the region Ω

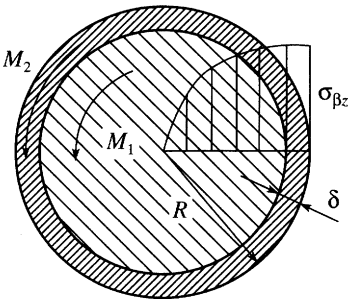

Fig. 1.

by summation over all the elements, we obtain a discrete analogue of the equations of motion for each node of the grid

$$(Mw_r)_j = (F_r)_j, \quad (w_r)_j = (\ddot{u}_r)_j - (r_M\dot{\theta}^2)_j$$
$$(J_z w_\beta)_j = (F_\beta)_j, \quad (w_\beta)_j = (r_J\ddot{\theta})_j + (2\dot{u}_r\dot{\theta})_j$$
$$(Mw_z)_j = (F_z)_j, \quad (w_z)_j = (\ddot{u}_z)_j; \quad j = 1, 2, \ldots, N \tag{1.6}$$

Here F_r, F_β, F_z are generalized forces, acting on the calculation node j, $r_M = M^r/M$, $r_J = J_z^r/J_z$ are weighting factors, M, M^r and J_z, J_z^r are generalized nodal masses and moments of inertia, and N is the number of nodes of the discrete model.

The process of deformation of a solid medium with time is split into time layers $t^0, t^1, \ldots, t^k, \ldots$ with steps $\Delta t^{k+1} = t^{k+1} - t^k$ When solving torsion–tension problems the contribution of the non-linear term $(2\dot{u}_r\dot{\theta}|)_j$ in relation (1.6) is negligibly small, that makes it possible to reduce the solution of the system of Eq. (1.6) to an explicit "cross" type scheme of integration over time. Finally, the rates of displacement, the displacement and the current coordinates of the nodes of the discrete model of a solid medium are found from the recurrence relations

$$\dot{\theta}_j^{k+1/2} = \dot{\theta}_j^{k-1/2} + (F_\beta^k)_j((J_z^r)_j^k)^{-1}\Delta t^{k+1/2}, \quad \theta_j^{k+1} = \theta_j^k + \dot{\theta}_j^{k+1/2}\Delta t^{k+1}$$
$$(\dot{u}_\alpha^{k+1/2})_j = (\dot{u}_\alpha^{k-1/2})_j + (F_\alpha^k + \nu(r_M(\dot{\theta}^{k+1/2})^2))_j(M_j)^{-1} \quad \Delta t^{k+1/2}$$
$$(u_\alpha^{k+1})_j = (u_\alpha^{k-1})_j + (\dot{u}_\alpha^{k+1/2})_j\Delta t^{k+1}, \quad \alpha_j^{k+1} = \alpha_j^0 + (u_\alpha^{k+1})_j; \quad \alpha = r, z, \quad j = 1, 2, \ldots, N$$
$$\nu = \begin{cases} 1, & \alpha = r \\ 0, & \alpha = z \end{cases}, \quad \Delta t^{k+1/2} = \frac{1}{2}(\Delta t^{k+1} + \Delta t^k)$$

Here the angular velocities of the nodes of the discrete model are first determined, and then the radial and axial velocities, taking the angular velocities obtained into account. The rates of displacement $(\dot{u}_\alpha^{k+1/2})_j$ and the angles of torsion $\dot{\theta}_j^{k+1/2}$ are calculated at the half-integer instants of time $(t^{k+1/2})$ and the displacements $(u_\alpha^{k+1/2})$ the angles of torsion θ_j^{k+1} and the coordinates α_j^{k+1} are calculated at the integer instants of time (t^{k+1}). The choice of the integration step in time Δt^{k+1} of the conditionally stable scheme (1.7) is made starting from the Courant stability condition.

2. The method of constructing strain diagrams when there is torsion

In numerical modelling, for the current angle of torsion of the sample we choose the cross-section with the greatest values of the stress intensity σ_i and the Odqvist parameter κ, at which the torque M is represented in the form of the sum of two moments of the shear stress $\sigma_{\beta z}$ in internal fibres M_1 and external fibres M_2 (Fig. 1)

$$M = 2\pi\int_0^{R-\delta}\sigma_{\beta z}r^2dr + 2\pi\int_{R-\delta}^{R}\sigma_{\beta z}r^2dr = M_1 + M_2 = M^{\exp} \tag{2.1}$$

Here R is the radius of cross-section, δ is the thickness of the external fibre and $M^{\exp} = M^{\exp}(\theta)$ is the experimental dependence of the value of the torque on the angle of torsion between the faces.

In torsion, the shear stress $\sigma_{\beta z}$ is a monotonically increasing function of the radius r and the time. We will assume that for this angle of torsion, the part of the strain diagram used to calculate the moment M_1 in the internal fibres $[0, R-\delta]$, has been obtained previously. The expression for the moment M_2, assuming that the thickness of the external fibre δ is small, can be written in the final form

$$M_2 = 2\pi\sigma_{\beta z}R^2\delta \tag{2.2}$$

The unknown shear stresses $\sigma_{\beta z}$ in the external fibres $[R-\delta, R]$ is found from relations (2.1) and (2.2)

$$\sigma_{\beta z} = (M^{\exp} - M_1)(2\pi R^2 \delta)^{-1} \tag{2.3}$$

The stresses obtained are used to construct the following section of the unknown part of the strain diagram $\sigma_i = \sigma_i(\kappa)$ from the formula

$$\sigma_i = \sqrt{\frac{3}{2}\sigma'_{ij}\sigma'_{ij}} \tag{2.4}$$

The Odqvist parameter is found from the last formula of (1.5).

In the general case of the torsion of an arbitrary solid of revolution, iterational refinement of the stress intensity and the Odqvist parameter is required. The stress intensity is corrected using the formula

$$\sigma_i = \sigma_i^*(\sigma_{\beta z}/\sigma^*_{\beta z}) \tag{2.5}$$

The quantity $\sigma_{\beta z}$ is found experimentally using formula (2.3), and σ_i^* and $\sigma^*_{\beta z}$ are calculated quantities. Extrapolation of the known part of the strain diagram is used as the initial approximation. The iterational correction procedure is carried out until the experimental and theoretical moments agree with a specified accuracy. Extrapolation also enables the strain diagram to be corrected, but not at each time step and only when the moments deviate more than a specified amount. The corresponding experimental dependence of the torque on the angle of torsion $M^{\exp} = M^{\exp}(\theta)$ is aligned with the strain diagram $\sigma_i = \sigma_i(\kappa)$ in a final single direct numerical calculation in discrete form with a specified accuracy.

To test the proposed procedure we constructed a strain diagram of 12Kh18N10T steel. The geometrical parameters of the sample (Fig. 2) are as follows: the radius and relative length of the working part $R_1 = 5$ mm and $L_1/R_1 = 20$, the relative radius and relative length of the clamped parts $R_2/R_1 = 1.65$ and $L_3/L_1 = 0.14$, and the overall length of the sample $L = 142$ mm.

In Fig. 2 the dash-dot curve represents the initial experimental relation $\hat{M}^{\exp} = M^{\exp}(R_1\theta/(2L_1))/M_T$ ($M_T = 2\cdot 3^{-3/2\pi}R_1^3\sigma_T$ is the limit plastic moment and $\sigma_T = 240$ MPa is the yield point); the continuous and dashed curves and the small circles represent the strain diagram $\hat{\sigma} = \sigma_i(\kappa)/\sigma_T$, constructed from experimental torsion data using this method, Ludwik's method[2] and experimental tension data[5] respectively.

The strain diagram constructed from experimental data on torsion and tension, practically agree, which confirms that the "stress intensity – Odqvist parameter" diagram is independent of the form of the stress state for large strains (up to 80%). For torsion, the uniformity of the stress-strain state along the working part of the sample is preserved until fracture, which enables the strain diagram to be constructed up to strains that are double those for tension.

3. Combined action of torsion and tension

We carried out a numerical and experimental investigation of the deformation of axisymmetric samples of variable thickness with a cylindrical working part under monotonic kinematic loading with torsion–tension, taking into account large deformations and the non-uniformity of the stress-strain state. The rate of loading was specified in such a way that the contribution of inertial forces were negligibly small.

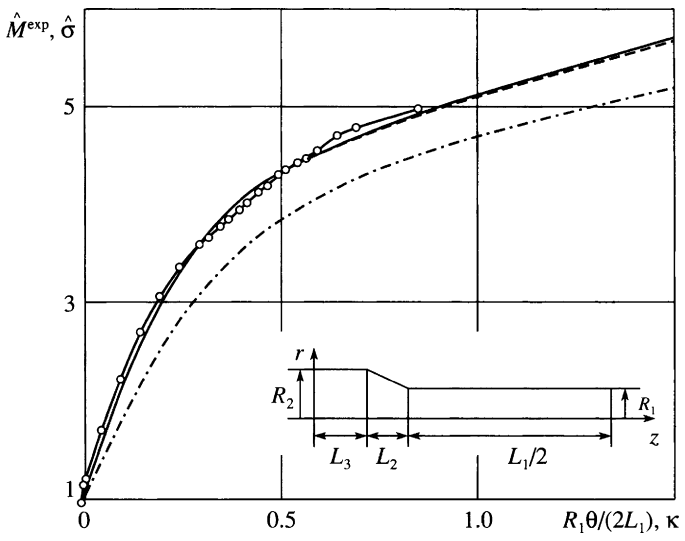

Fig. 2.

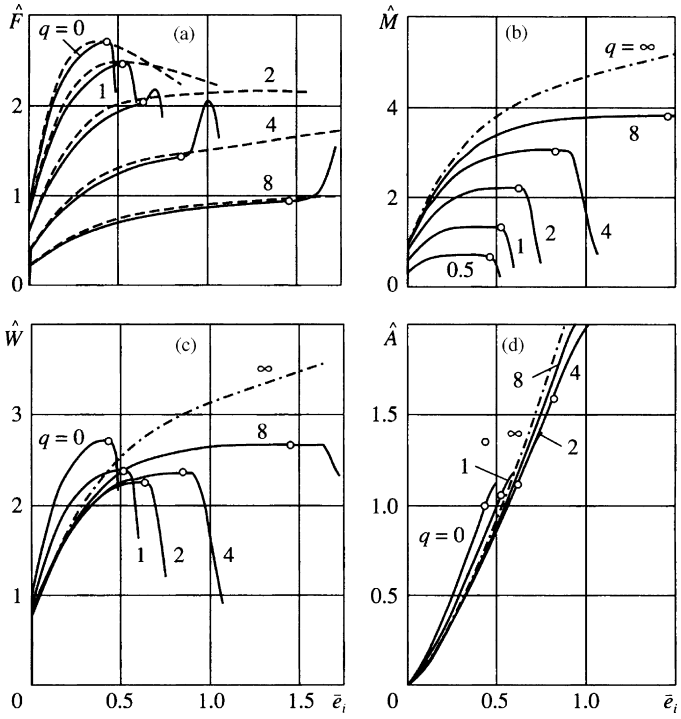

Fig. 3.

To estimate the neutral influence of the two forms of loading on the strain process we introduce the following parameters

$$q = \frac{R_1\theta}{\sqrt{3}u_z}, \quad \bar{e}_i = \sqrt{\bar{e}_{zz}^2 + \frac{4}{3}\bar{e}_{\beta z}^2} = \frac{u_z}{L_0}\sqrt{1+q^2}, \quad \bar{e}_{zz} = \frac{u_z}{L_0}, \quad \bar{e}_{\beta z} = \frac{1}{2}\frac{R_1\theta}{L_0}; \quad L_0 = \frac{L_1}{2}$$

$$F = 2\pi\int_0^R \sigma_{zz} r dr, \quad M = 2\pi\int_0^R \sigma_{\beta z} r^2 dr, \quad A = \int_0^{u_z} F du_z + \int_0^{\theta} M d\theta \tag{3.1}$$

The kinematic parameter q represents the "fraction of torsion and tension", $\bar{e}_i$, $\bar{e}_{zz}$ and $\bar{e}_{\beta z}$ are the conventional deformation intensity, axial and shear deformations respectively on the surface of the working part of the sample, referred to the initial length L_1 and radius R_1 of the working part of the sample, and u_z and θ are the axial displacement and angle of torsion between the end faces. For pure torsion $q = \infty$, $\bar{e}_i = 2\bar{e}_{\beta z}/\sqrt{3}$, for uniaxial tension $q = 0$, $\bar{e}_i = \bar{e}_{zz}$, and for combined loading $0 < q < \infty$; F is the axial force, M is the torque and A is the total work of the axial force and the torque.

Assuming $q \equiv$ const, the expression for the work can be converted to the form (W is the generalized force)

$$A = \int_0^{\bar{e}_i} \frac{L_0}{\sqrt{1+q^2}}\left(F + \frac{\sqrt{3}q}{R_1}M\right)d\bar{e}_i = \int_0^{\bar{e}_i} W d\bar{e}_i \tag{3.2}$$

In Fig. 3 we show graphs of the dimensionless force parameters against the conventional deformation intensity $\bar{e}_i$: the axial force $\hat{F} = F/F_T (F_T = \pi R_1^2 \sigma_T)$, the torque $\hat{M} = M/M_T$, the generalized force $\hat{W} = W/W_T (W_T = L_0 F_T)$ and the total work of the axial force and the torque $\hat{A} = A/\tilde{A}$ ($\tilde{A}$ is the work done by the axial force during tension up to the instant when a neck forms) for various values of the parameter q.

We will take as the criterion of loss of stability of plastic deformation, with the formation of a neck, the condition $d\hat{W}/d\bar{e}_i = 0$, which characterises the instant when the generalized force $\hat{W}$ reaches its maximum values, denoted by the points on the curves. The inflection points on the graphs of the work $\hat{A}(\bar{e}_i)$ in Fig. 3,d correspond to these. After the instant of loss of stability in the case when, during loading, tension prevails $0 \le q < 1$, an intensive reduction in the force parameters is observed. In the case when torsion predominates $1 \le q < \infty$, the maximum values of the axial force $\hat{F}$ are reached after the instant of loss of stability during the formation of the neck, when the value of the torque $\hat{M}$ is reduced due to the reduction in the radius of cross-section of the neck.

The sharp change in the integral characteristics is due to the fact that the conventional deformation intensity $\bar{e}_i$ does not take into account the local change in the geometrical parameters of the sample. The increase in the axial force $\hat{F}$ as a function of the Odqvist parameter κ in the neck on the surface of the sample occurs smoothly, and after the instant when loss of stability occurs (the dashed curves in Fig. 3,a).

The legitimacy of using the criterion of the loss of stability of plastic deformation for a combined load considered above is confirmed by the distribution of the Odqvist parameter κ along the surface of the sample, shown in Fig. 4. The dashed curves correspond to the instant when the generalized force $\hat{W}$ reaches the maximum values, while the continuous curves represent the instant when the Odqvist

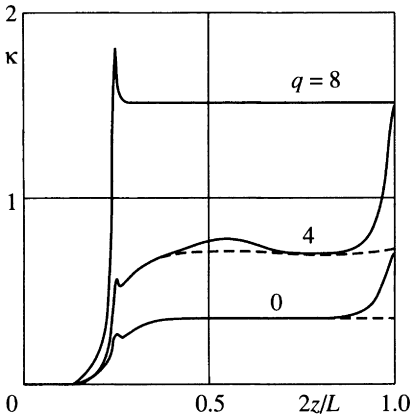

Fig. 4.

parameter reaches the maximum values: for pure torsion $\kappa = 1.5$, for uniaxial tension $\kappa = 0.7$ in the neck, and for combined loading $\kappa = 1.5$ in the neck. When $q = 0$ and $q = 4$, after the generalized force $\hat{W}$ reaches the critical (maximum) values a neck is formed in the region of the plane of symmetry, as a result of which intensive local increase in the Odqvist parameter is observed. At the point where the thickness of the sample changes, a concentration of stresses and deformations occurs, which, in the experiment on torsion $q = \infty$, leads to a transverse shear in this section when $\kappa = 1.5$ on the surface of the sample.

The deformation up to the instant when there is loss stability are close to radial, while the supercritical behaviour is characterized by trajectories of small curvature. For combined loading ($0 < q < \infty$) before the instant of loss of stability over the whole volume of the sample the form of the stress state changes slowly towards tension, since the sample has thinned out. The change in the form of the stress state in the neck towards shear, after the instant of loss of stability, occurs most intensively for pure tension ($q = 0$).

Before the axial force over the whole volume of the sample decreases, a process of active loading occurs. At the point where the neck is formed, the active process continues up to fracture. In experiments, the neck is formed in the middle part of the sample, and its position

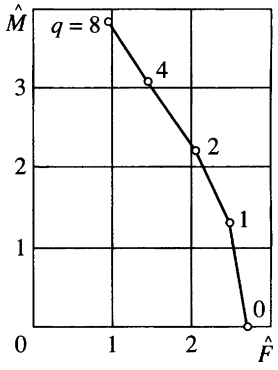

Fig. 5.

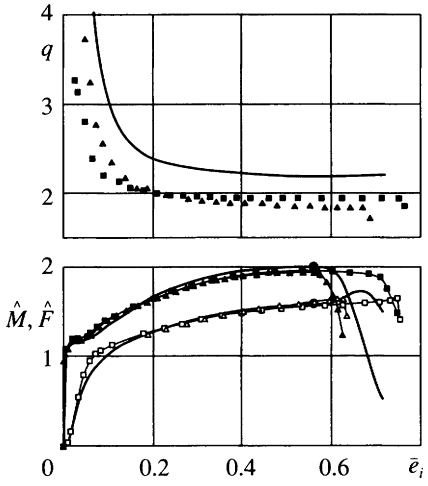

Fig. 6.

depends on many random factors. In calculations the initial radius of the sample close to the plane of symmetry was $0.999R_1$, which led to the formation of a neck in the plane of symmetry. For the combined action of torsion and tension, the neck is less pronounced than for tension alone. For uniaxial tension, numerical and experimental results agree well both as regards the limit load and as regards the shape and dimensions of the neck.[5]

In Fig. 5 we show the region of stability of plastic deformation when torsion and tension act together. For pure torsion, there is no loss of stability of plastic deformation with the formation of a neck. As a consequence of this, the line separating the regions of stable and unstable deformation has an inflection paint, and, when the fraction of torsion increases ($q \to \infty$), it approaches the ordinate axis asymptotically.

In Fig. 6 we compare the results of a calculation (the continuous curve) with experimental data (the triangles and squares) with respect to the parameter q, the torque $\hat{M}$ and the axial force $\hat{F}$. The features of the sample deformation processes observed in the experiment agree well with the theoretical investigations (Fig. 3) after the proportional loading regime has been established ($q \approx 2$) up to the instant of loss of stability of plastic deformation with the formation of a neck (denoted by points in the figure).

Acknowledgements

We wish to thank our colleagues A. S. Gorokhov and D. A. Kazakov at the Scientific Research Institute of Mechanics of the N. I. Lobachevskii Nizhegorod State University for their help in carrying out the experiments.

This research was financed by the Russian Foundation for Basic Research (05-0100837) and the Programme for the Support of Leading Scientific Schools (NSh-6391.2006.8).

References

1. Degtyarev VP. *Deformation and Fracture in Highly Stressed Structures*. Moscow: Mashinostroyeniye; 1987.
2. Nadai A. *Theory of Flow and Fracture of Solids*. N.Y. etc.: McGraw-Hill; 1963.
3. Vasin RA, Il'yushin AA, Mossakovskii PA. Investigation of the constitutive relations and fracture criteria for solid and thin-walled tubular cylindrical samples. *Izv Ross Akad Nauk MTT* 1994;**2**:177–84.
4. Bazhenov VG, Zefirov SV, Kibets AI. The numerical realization of the variational-difference moment scheme for solving non-linear problems of the dynamics of thick shells under impulsive forces. In: *Applied Strength and Plasticity Problems. Methods of Solution*. Gor'kii: Izd Gor'k Univ; 1988. p. 66–73.
5. Bazhenov VG, Kibets AI, Laptev, Osetrov SL. An experimental-theoretical investigation of the limit states of elastoplastic rods of various cross-section under tension. In: Klimov DM, et al., editors. *Problems of Mechanics. Collected Papers Celebrating the 90th Birthday of A. Yu. Ishlinskii*. Moscow: Fizmatlit; 2003. p. 115–22.

Translated by R.C.G.